Three-dimensional magnetic focusing of particles and cells in ferrofluid flow through a straight microchannel

2012 J. Micromech. Microeng. 22 105018

(http://iopscience.iop.org/0960-1317/22/10/105018)

J. Micromech. Microeng. **22** (2012) 105018 (8pp) doi:10.1088/0960-1317/22/10/105018

Three-dimensional magnetic focusing of particles and cells in ferrofluid flow through a straight microchannel

Jian Zeng[1], **Chen Chen**[1], **Pallavi Vedantam**[2], **Vincent Brown**[1], **Tzuen-Rong J Tzeng**[2] **and Xiangchun Xuan**[1,3]

[1] Department of Mechanical Engineering, Clemson University, Clemson, SC 29634-0921, USA
[2] Department of Biological Sciences, Clemson University, Clemson, SC 29634-0314, USA

E-mail: xcxuan@clemson.edu

Received 12 June 2012, in final form 18 July 2012
Published 28 August 2012
Online at stacks.iop.org/JMM/22/105018

Abstract

Focusing particles and cells into a tight stream is often required in order for continuous flow detection, counting and sorting. So far a variety of particle focusing methods have been developed in microfluidic devices, among which magnetic focusing is still relatively new. We develop in this work an approach to embedding symmetrically two repulsive permanent magnets about a straight rectangular microchannel in a PDMS-based microfluidic device. The closest distance between the magnets is limited only by the sizes of the embedded and holder magnets involved in the fabrication process. The developed device is used to implement and investigate the three-dimensional magnetic focusing of polystyrene particles in ferrofluid microflow with both the top- and side-view visualizations. The effects of flow speed and particle size on the particle focusing effectiveness are studied. The developed device is also applied to magnetically focus yeast cells in ferrofluid, which proves to be biocompatible as verified by a cell viability test. In addition, an analytical model is developed and found to be able to predict the experimentally observed particle and cell focusing behaviors with reasonable agreement.

(Some figures may appear in colour only in the online journal)

1. Introduction

Focusing particles and cells into a tight stream is often required in order to continuously detect, count and sort them for chemical and biomedical applications [1–3]. A variety of particle focusing methods have been developed in microfluidic devices, which rely on either sheath fluid(s) (i.e., sheath flow focusing) [4–9] or lateral force(s) (i.e., sheathless focusing) to manipulate the suspending fluid or the suspended particles for transverse particle movement [10–12]. The latter can be further classified as active and passive based on if the force field is externally applied or internally induced [13]. Active particle focusing methods involve an optical [14], acoustic [15, 16], electric [17] and dielectrophoretic [18, 19] force that acts directly on the suspended particles and moves them to the position of nil force. Passive particle focusing methods exploit the fluid and/or channel structure-induced inertial [20, 21], hydrodynamic [22, 23], viscoelastic [24, 25] and dielectrophoretic [26, 27] effects to manipulate particles to equilibrium positions.

Magnetic approach to particle and cell focusing is relatively new though it has clear advantages over other methods such as low cost, noninvasive, free of fluid heating issues (if permanent magnets are used), independence of fluid and channel properties, etc [28–30]. This approach utilizes magnetophoresis to direct particles either along (i.e. positive magnetophoresis) [31–33] or against (i.e. negative magnetophoresis) [34–37] a magnetic field gradient. The former case takes place when magnetic particles (either intrinsically magnetic or magnetically tagged) are suspended in diamagnetic solutions. In this direction Afshar *et al* [38] demonstrated a three-dimensional focusing of magnetic

[3] Author to whom any correspondence should be addressed.

particles in a diamagnetic aqueous medium by first trapping the particles against the channel sidewall closer to an electromagnetic tip and then pushing them to the channel center with a sheath flow. However, the majority of synthetic and biological particles are intrinsically diamagnetic. Like all other diamagnetic materials, these particles experience a repulsive force from a magnetic field [28–33]. Such negative magnetophoretic motion can be enhanced if the diamagnetic particles are suspended in magnetic solutions. In this direction Xuan's group [39] has recently employed a similar design to that of Afshar *et al* [38] for focusing diamagnetic particles in ferrofluid, where the particles are focused to a tight stream along the interface of the ferrofluid and sheath water in a T-shaped microchannel. A single permanent magnet is embedded adjacent to the microchannel, which significantly enhances the magnetic field and field gradient enabling a label-free (i.e. no magnetic or fluorescent labeling) particle focusing in a very dilute ferrofluid.

There are also a few other papers that have reported the use of negative magnetophoresis for continuous focusing of diamagnetic particles and cells in magnetic fluids [40–42]. In these papers a pair of opposing magnets was used to create magnetic field gradient null at the center of a micro conduit. Specifically Pamme's group [40, 41] studied the magnetic focusing of both polystyrene particles and mammalian cells in paramagnetic solutions (of various concentrations), where a specialized mechanical setup was employed to precisely align two facing magnets about a circular micro capillary. Mao's group [42] conducted a combined experimental and theoretical study of the magnetic focusing of polystyrene particles in ferrofluid flow through an on-chip rectangular microchannel. Two long magnets of 7 mm apart were embedded into the polydimethylsiloxane (PDMS) layer, which was found insufficient to focus 5 μm particles into a single line in their channel. The focused particle stream was still about 100 μm wide at the lowest tested speed (about 100 μm s^{-1} as calculated from the given flow rate) [42]. Additionally Koser's group demonstrated a simultaneous focusing of multiple sizes of particles in their ferrofluid-mediated nanocytometer, which utilizes a low-cost electrode substrate to create locally programmable magnetic fields [43].

In this work we develop an approach to embedding two repulsive permanent magnets into a PDMS-based microfluidic device. The closet distance between the magnets is limited only by the sizes of the embedded and holder magnets involved in the fabrication process, which, as shown later, is more than twice smaller than that achieved by Mao's group [42] and can be further reduced. This developed device is used to investigate the magnetic focusing of polystyrene particles in ferrofluid in both the horizontal and vertical planes of a straight microchannel with the top- and side-view visualizations. Due to the induced negative magnetophoresis, diamagnetic particles are deflected across the ferrofluid and focused to a narrow stream flowing near the bottom edge of the channel center plane. The same device is also applied to test the feasibility of magnetic focusing of live cells in ferrofluid. In addition a theoretical model is developed to simulate the magnetic focusing of diamagnetic particles and cells in ferrofluid microflow.

2. Experiment

2.1. Device fabrication

The microchannel was fabricated with PDMS by the method of standard soft lithography [39, 44, 45]. To create the microchannel master, photoresist (SU-8, MicroChem Corp., Newton, MA) was dispensed on an acetone-treated glass slide and spun (WS-400E-NPP-Lite, Laurell Technologies, North Wales, PA) at a terminal speed of 800 rpm. Then, the slide was heated on a hot plate (HP30A, Torrey Pines Scientific, San Marcos, CA) at 65 °C for 5 min and 95 °C for 15 min as part of the process of a soft bake. Following that, a photomask (designed using AutoCAD® and printed on a transparent film) was placed on top of the slide and the photoresist film underwent UV exposure (ABM Inc., San Jose, CA) at a prescribed dose. Next, a postexposure baking of the slide occurred at 65 °C for 1 min and 95 °C for 4 min. Once baking was complete, the photoresist was immersed in SU-8 developer solution for 6 min. Finally, the photoresist was rinsed using isopropyl alcohol and allowed to dry at room temperature. The processed photoresist leaves a positive indentation of the microchannel geometry and is ready to be used for channel fabrication.

In order to embed two opposing Neodymium–Iron–Boron (NdFeB) permanent magnets (B222, $1/8'' \times 1/8'' \times 1/8''$, K&J Magnets, Inc.) into the PDMS layer, three top magnets (two B222 and one B224, $1/8'' \times 1/8'' \times 1/4''$) and three bottom magnets (B421, $1/4'' \times 1/8'' \times 1/16''$, K&J Magnets, Inc.) were used to fix the magnet positions. The three bottom holder magnets were placed below a petri dish, having the dish and glass slide between the embedded and holder magnets. The three top holder magnets were placed in direct contact with the embedded ones. A picture of thus arranged magnets is shown in figure 1(*a*), where the north and south poles of the embedded magnets are labeled. The inset of figure 1(*a*) illustrates how the magnetic poles of the embedded and holder magnets are configured to form a stable holding. The distance between the two embedded magnets is determined by the dimensions of both the holder and the embedded magnets. A right-angle prism (NT32–526, Edmund Optics Inc.) was placed 700 μm away from the microchannel and 5 mm downstream of the magnets for side viewing. It was fixed onto the glass slide using sticky tape (see figure 1(*a*)).

Once the prism and magnets were in place, liquid PDMS was dispensed to the dish and underwent degassing in an isotemp vacuum oven (13-262-280A, Fisher Scientific, Fair Lawn, NJ) for 30 min. Afterward, the dish was moved into a gravity convection oven (13-246-506GA, Fisher Scientific, Fair Lawn, NJ) for curing at 65 °C for 3 h. Following that, the holder magnets were removed and the PDMS was cut out and punched with two through holes at the designed locations. Finally the PDMS slab was bonded to a glass slide after plasma treating (PDC-32G, Harrick Scientific, Ossining, NY) for 1 min. Figure 1(*b*) shows a picture of the microfluidic device used in our experiments. The straight microchannel is 2 cm long and has a uniform cross-section of 600 μm (width) by 60 μm (depth). The two embedded opposing magnets are symmetric about the microchannel with an edge-to-edge

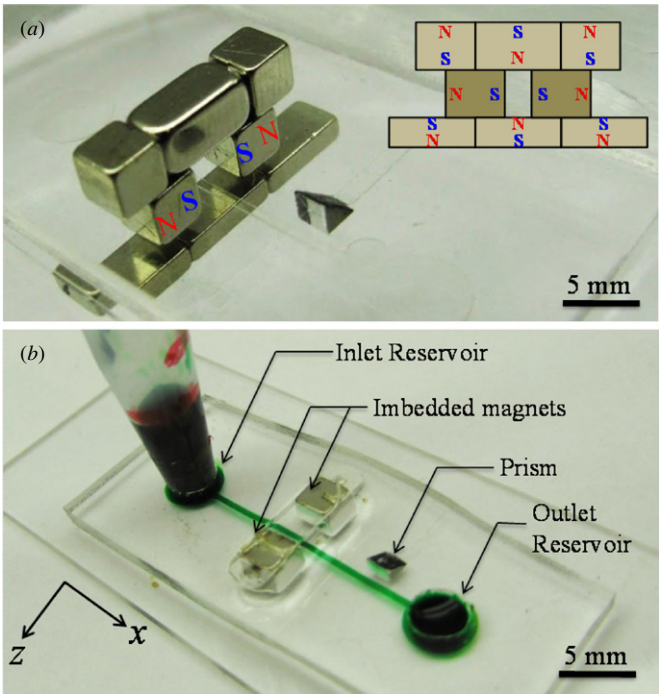

Figure 1. (*a*) Picture of the placed magnets and prism prior to the dispensing of liquid PDMS, where the inset shows how the magnetic poles of the embedded (middle row) and holder (top and bottom rows) magnets are configured to form a stable holding; (*b*) picture of the microfluidic device (the microchannel and reservoirs are filled with green food dye for clarity) used in the experiment. The origin of the coordinate system in (*b*) is at the center of the microchannel inlet with the *y*-axis pointing upward (i.e. opposite to the gravity direction).

distance of 3.1 mm. This distance is roughly the size of the embedded magnet (1/8″) and can be further reduced if smaller magnets (e.g., B111, 1/16″ × 1/16″ × 1/16″, K&J Magnets, Inc.) are used.

2.2. Particle and cell solutions preparations

A water-based ferrofluid, EMG 408, was obtained from Ferrotec (USA) Corp., which consists of 1.2% magnetic nanoparticles (10 nm diameter) by volume with a manufacturer identified saturation magnetization of 6.6 mT and viscosity of 2 mPa s. Green fluorescent polystyrene particles of 5 μm diameter from Duke Scientific Corp. were originally packaged as 1% solids in water with size nonuniformity of 5% at most. By dilution using deionized water, the final particulate solution used in experiment was 0.25 × the original EMG 408 ferrofluid suspended with 5×10^6 particles ml^{-1}. For the experiment on a particle mixture, 1 μm green fluorescent polystyrene particles from Bangs Laboratory were directly suspended into the 5 μm particle solution to a concentration of 5×10^7 particles ml^{-1}.

Yeast cells (*Saccharomyces cerevisiae*) were cultured overnight in Sabouraud's dextrose broth in a shaker incubator at 30 °C, and were resuspended in sterile phosphate buffered saline (PBS) solution to a concentration of 5.73×10^8 cells ml^{-1}. In order to stain the live cells, 1 μl ml^{-1} of SYTO 9 green fluorescent stain (Molecular Probes) was added to the yeast cell suspension. Prior to use, the stained yeast cells were washed with deionized water three times then resuspended in 0.25 × EMG 408 ferrofluid to a final concentration of around 5×10^6 cells ml^{-1}. The measured diameter of yeast cells is 5 μm on average. Tween 20 (Fisher Scientific) was added to both the particle and cell suspensions at 0.1% by volume to minimize (or prevent) their aggregations and adhesions to microchannel walls.

2.3. Particle/cell manipulation and visualization

The particle or cell suspension in ferrofluid was driven through the microchannel by adjusting the liquid height difference between the inlet and outlet reservoirs. A regular 1 ml pipette tip was inserted into the through hole in the PDMS slab serving as the inlet reservoir. Prior to experiment the solution in the outlet reservoir was vacated. The liquid height in the inlet reservoir was varied to achieve different flow speeds, which were first estimated through theoretical calculation and then verified via experimental tracking of individual particles [39, 44]. The visualization of particle/cell motion was achieved using an inverted microscope (Nikon Eclipse TE2000U, Nikon Instruments, Lewisville, TX) equipped with a CCD camera (Nikon DS-Qi1Mc). Videos and images were recorded and processed using the Nikon imaging software (NIS-Elements AR 2.30).

3. Theory

3.1. Mechanism of diamagnetic particle focusing in ferrofluid

Diamagnetic particles suspended in ferrofluid experience a magnetic force inside a nonuniform magnetic field, which deflects them away from the high field region at velocity, $\mathbf{U}_m$ [45]:

$$\mathbf{U}_m = \frac{-\mu_0 \phi a^2}{9\eta f_D} \frac{M_d L(\alpha) \nabla \mathbf{H}^2}{H} \tag{1}$$

$$L(\alpha) = \coth(\alpha) - \frac{1}{\alpha} \text{ and } \alpha = \frac{\pi \mu_0 M_d H d^3}{6 k_B T}. \tag{2}$$

In the above, μ_0 is the permeability of free space, ϕ is the volume fraction of magnetic nanoparticles in the ferrofluid, a is the radius of diamagnetic particles, η is the ferrofluid viscosity, f_D is the drag coefficient to account for the particle-wall interactions [42, 44–47], M_d is the saturation moment of magnetic nanoparticles, $L(\alpha)$ represents Langevin function [48], $\mathbf{H}$ is the magnetic field with a magnitude of H, d is the average diameter of magnetic nanoparticles, k_B is the Boltzmann constant and T is the ferrofluid temperature. Note that the contribution of the magnetization of diamagnetic particles has been neglected in equation (1) because it is usually much smaller than that of the ferrofluid. For the magnetic field produced by a block magnet Furlani's analytical model [49] can be applied if the ferrofluid is assumed to have a negligible effect on the magnetic field distribution. This has been proved reasonable in several recent studies [42, 44–47].

The use of two opposing magnets of equal geometry and magnetization (see figure 1(*b*)) can create a nonuniform

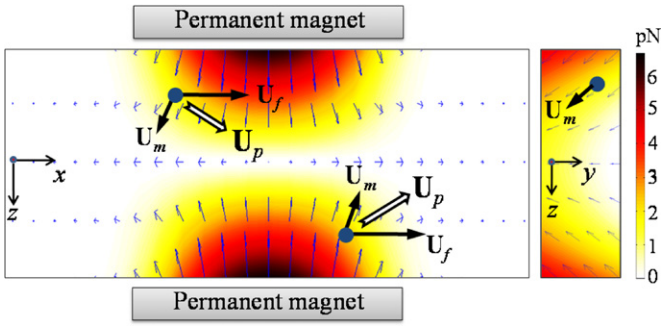

Figure 2. Velocity analysis of a diamagnetic particle suspended in a ferrofluid in the horizontal (left plot) and vertical (right plot) planes of the microchannel when subjected to the nonuniform magnetic field of two opposing magnets (not drawn to scale). The background color and arrows display the contour and the vector distribution of the magnetic force experienced by the particle.

but symmetric magnetic field within the microchannel in the horizontal plane, where the minimum field occurs right along the channel centerline [40–42]. Therefore, diamagnetic particles are pushed horizontally away from the channel wall by magnetic force at velocity, $\mathbf{U}_m$, as they pass the magnet region along with the ferrofluid flow at velocity, $\mathbf{U}_f$. This is illustrated by the vector distribution of the magnetic force and the analysis of the particle velocity, $\mathbf{U}_p = \mathbf{U}_f + \mathbf{U}_m$, in figure 2 (left plot, see also the contour of the magnetic force magnitude). Moreover, the two opposing magnets also generate magnetic field gradients in the vertical plane [39, 45], inducing a magnetic force on the particle toward the bottom wall of the microchannel; see the force vector and the induced magnetophoretic particle velocity in the right plot of figure 2.

The combined effect of the magnetically induced horizontal and vertical particle deflections is a focused particle stream near the bottom edge of the channel mid-plane. The effectiveness of such 'three-dimensional' magnetic focusing can be simply measured by the ratio of the particle velocity perpendicular and parallel to the flow direction:

$$\text{Focusing} \propto \frac{U_{p,i}}{U_{p,x}} = \frac{U_{m,i}}{U_f + U_{m,x}} \approx \frac{U_{m,i}}{U_f} \quad (i = y, z) \tag{3}$$

where $U_{p,i}$ $(i = x, y, z)$ denotes the particle speed in the directions of fluid flow (x), channel depth (y) and channel width (z), respectively, $U_{m,i}$ is the magnetophoretic particle speed in each of the three directions (refer to equation (1) for the magnetophoretic velocity) and U_f is the ferrofluid flow speed. Note that the gravity induced particle sedimentation in the channel depth direction (y) is neglected in the last equation. This is justified by the close match of the mass densities of the ferrofluid (about 1.03 g cm^{-3} for 0.25 × EMG 408) and the particle (1.05 g cm^{-3}), which leads to a sedimentation speed of 0.27 μm s^{-1} at most. Equation (3) along with equation (1) indicates that the diamagnetic particle focusing can be enhanced by increasing the particle size and ferrofluid concentration or decreasing the ferrofluid flow speed. Moreover, bringing closer the two opposing magnets can increase the magnetic field and gradients and hence enhance the particle focusing. In addition, using a longer magnet in the flow direction should also be beneficial as demonstrated by Mao's group [42].

3.2. Simulation of particle trajectory

The analytical model that we developed in earlier works [44, 45] was used to simulate the three-dimensional diamagnetic particle focusing in our experiments. The magnetic field distribution was obtained by superimposing the magnetic fields of the two opposing magnets, which was each computed from Furlani's analytical formula [49] and neglected here for conciseness. The diamagnetic particle was assumed massless and had the velocity, $\mathbf{U}_p = \mathbf{U}_f + \mathbf{U}_m$, as explained above (see figure 2). The ferrofluid flow in the straight microchannel was assumed fully developed and not affected by particle magnetophoresis. The flow velocity was assumed to follow the analytical formula for pressure-driven flow in a rectangular channel. The applied pressure drop across the channel was estimated from hydrostatic pressure by measuring the height difference of the liquid columns in the inlet and outlet reservoirs. The instantaneous position of the particle center was computed by integrating $\mathbf{U}_p$ over time with respect to its initial position, which was performed in Matlab®. The technical detail of the model implementation in Matlab® is referred to Liang *et al* [45].

4. Results and discussion

4.1. 3D magnetic focusing of 5 μm particles

The three-dimensional magnetic focusing of 5 μm polystyrene particles was studied in 0.25 × EMG 408 ferrofluid at a mean flow speed of 0.4 mm s^{-1} (or equivalently a flow rate of 0.85 μl min^{-1}). This focusing in the horizontal plane of the microchannel (i.e. the channel width direction in top view) was visualized with videos recorded at two view windows along the channel length; see the schematic (not to scale) on the top of figure 3. The first window is centered at the leading edge of the magnets relative to the fluid flow and the second window is about 5 mm downstream of the magnets' back edge. Figure 3(*a*) presents the snapshot image (top), superimposed image (middle) and simulated particle trajectories (bottom) from the top view of each of these two locations. Note that the original images have been cropped and adjusted (in both contrast and brightness) for best view. The superimposed image was obtained by superimposing a sequence of more than 200 snapshot images over a 20 s timeframe. The horizontal focusing of 5 μm particles can be clearly seen in figure 3(*a*1) as the particles enter the magnet region with a nearly uniform distribution over the channel width and begin to get pinched toward the center of the microchannel by negative magnetophoresis.

Downstream from the magnets, the laminar flow allows for the magnetically deflected particles to remain in their positions relative to the width of the channel. As demonstrated in figure 3(*a*2), particles move along the channel centerline in almost a single file (see the snapshot image in the top). The measured width of this focused particle stream (see the superimposed image in the middle) is 35 μm, which

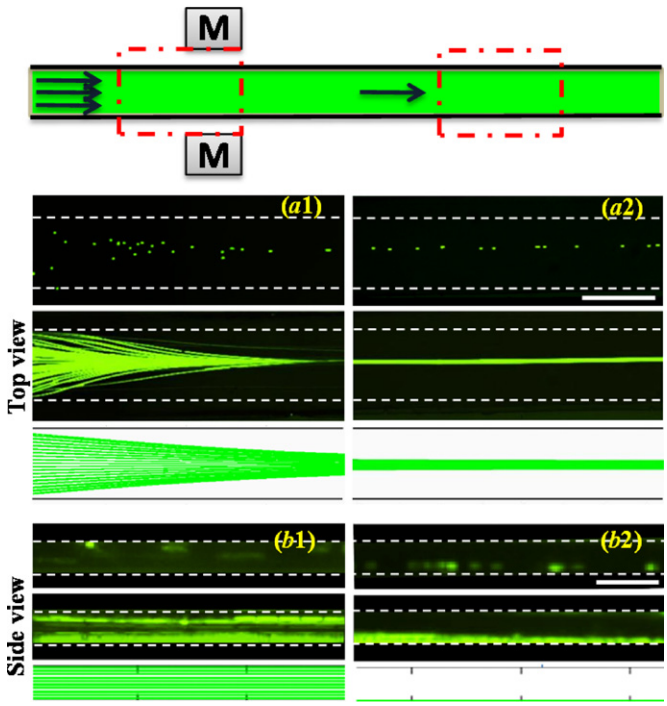

Figure 3. Experimental and theoretical results illustrate the three-dimensional magnetic focusing of 5 μm diamagnetic particles in 0.25 × EMG ferrofluid through a straight microchannel at a mean flow speed of 0.4 mm s^{-1}: top views from the view windows (see their locations relative to the magnets in the schematic on the top of the figure) at the front edge of the magnets (a1) and 5 mm downstream of the back edge of the magnets (a2); side views from the view window before the magnets (b1) and after the magnets (b2). The top, middle and bottom plots in each panel (i.e. (a1), (a2), (b1) and (b2)) show the experimentally obtained snapshot and superimposed images and the theoretically simulated particle trajectories, respectively. The flow direction is from left to right in all images. The scale bars in (a2) and (b2) represent 600 μm and 60 μm, respectively.

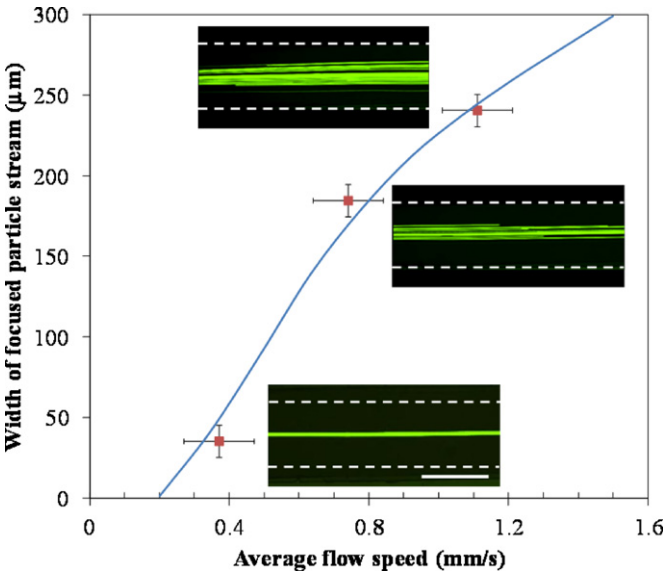

Figure 4. Ferrofluid flow speed effect on the magnetic focusing of 5 μm particles in the horizontal plane of the microchannel. The symbols with error bars represent the experimentally measured particle stream widths at the flow speeds of 0.4 mm s^{-1}, 0.8 mm s^{-1} and 1.2 mm s^{-1}, respectively. The solid line is the theoretically predicted curve from the analytical model. The flow direction is from left to right in all the insets (superimposed particle images). The scale bar represents 600 μm.

appears to be much wider than the particle diameter (5 μm). This is because fluorescent particles look apparently larger than their real sizes in recorded images. These observed magnetic pinching and focusing behaviors of particles in the channel width direction are reasonably captured by the theoretical model (see the middle and bottom rows in figure 3(a)). However, the model seems to underpredict the particle focusing performance. This discrepancy may be due to the error in measuring the liquid height difference in the inlet and outlet reservoirs, which affects the ferrofluid flow speed and hence the particle focusing, see equation (3).

The magnetic focusing of 5 μm particles in the vertical plane of the microchannel (i.e., the channel depth direction in side view) was visualized through the use of the embedded prism and is demonstrated in figure 3(b). The unfocused particle images in figure 3(b1) were obtained when the ferrofluid flow direction in the microchannel was reversed. In other words, the prism shown in figure 2 became actually located at the upstream of the magnets where particles were not magnetically deflected. In contrast, figure 3(b2) shows the snapshot (top) and superimposed (middle) images of particles that have been vertically focused by the induced negative magnetophoresis in ferrofluid. As expected, the particles occupy the bottom surface of the channel [39, 45] and migrate through the view window in a single file, which is also reasonably predicted by the theoretical model. Note that the particles in the side-view images look dim relative to those in the top-view images due to the optical interferences from the prism and its interfaces with PDMS.

4.2. Flow speed effect on magnetic focusing of 5 μm particles

The effect of ferrofluid flow speed on the magnetic focusing of 5 μm particles is presented in figure 4. All parameters remain similar to those in figure 3 during the test except that the flow speed is varied from 0.4 mm s^{-1} to 0.8 mm s^{-1} and 1.2 mm s^{-1}. Consistent with equation (3) that predicts a weaker focusing of particles suspended in a faster flow, the measured width of the focused particle stream (symbols with error bars in figure 4) increases with the flow speed. This is because the faster the particles move, the less time they get exposed to the magnetic field gradient and hence experience less magnetic deflection. The inset images in figure 4 illustrate the superimposed particle images at the three tested flow speeds, which are all obtained at the view window 5 mm downstream of the back edge of the magnets. One can see in figure 4 that the experimentally measured particle stream widths (symbols with error bars) agree closely with the theoretically predicted curve (solid line) within the experimental errors (10 μm for the error of measured stream width and 0.1 mm s^{-1} for the error of measured flow speed).

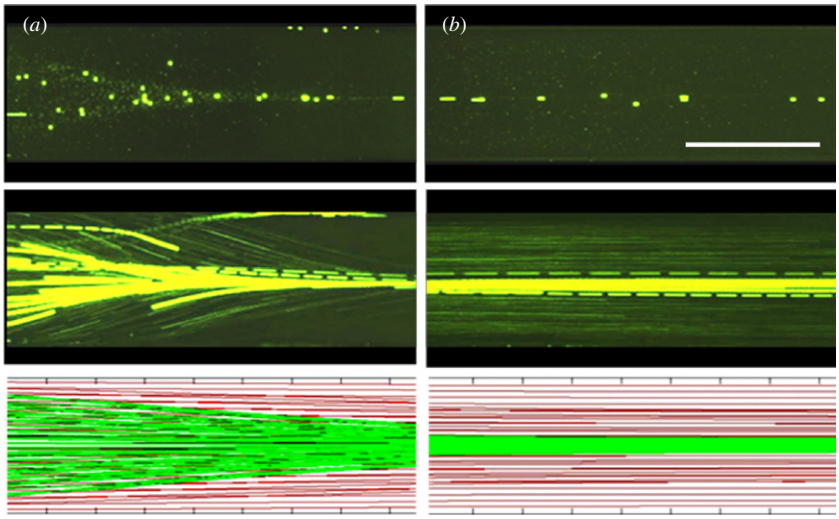

Figure 5. Experimental (top and middle rows) and theoretical (bottom row) results for the magnetic focusing of 5 μm and 1 μm particle mixture in ferrofluid microflow: top views from the view window at the front edge of the magnets (*a*) and the view window 5 mm downstream of the back edge of the magnets (*b*). The green (darker lines close to the channel center) and red lines in the simulation images (bottom row) represent the trajectories of 5 μm and 1 μm particles, respectively. The experimental conditions and the image layout are similar to figure 3. The flow direction is from left to right. The scale bar represents 600 μm.

4.3. Magnetic focusing of 5 μm and 1 μm particle mixture

Figure 5 illustrates the magnetic focusing of 5 μm and 1 μm particle mixture in ferrofluid flow through the straight microchannel. The purpose of this experiment is twofold: one is to examine the effect of the presence of other particles (of dissimilar properties, here, of different sizes) on diamagnetic particle focusing, and the other is to demonstrate the particle size dependence of this focusing approach. The experimental conditions are the same as those in figure 3. The layout of the images from the two view windows shown in figure 5 is also identical to that in figure 3. One can see in figure 5(*a*) that as the particle mixture enters the magnets region 5 μm particles undertake a much greater magnetic deflection than 1 μm ones. This is consistent with equation (1), which predicts a quadratic dependence of the induced magnetophoretic velocity on particle diameter. The result is that 5 μm particles are focused into a tight stream along the channel centerline while 1 μm particles are still distributed across the majority of the channel width as demonstrated in figure 5(*b*). Moreover, the focusing of 5 μm particles appears similar to that shown in figure 3, indicating an insignificant influence from the presence of 1 μm particles. These observed particle behaviors are properly captured by the theoretical model, where the green and red lines in figure 5 (bottom row) represent the trajectories of 5 μm and 1 μm particles, respectively. Such distinct motions of the two sizes of particles are envisioned to enable a continuous concentration and filtration of particles by size.

4.4. Magnetic focusing of yeast cells

We also investigated the magnetic focusing of live yeast cells in ferrofluid flow through the fabricated straight microchannel. As the cells have an average diameter of 5 μm, similar experimental conditions to those for 5 μm polymer particles (see section 4.1.) are used for this test. Figure 6 shows the top-view superimposed cell images obtained from the two view windows as noted in figure 3. Snapshot images are not presented here due to the stained cells being far dimmer than fluorescent particles. The same pinching effect for the particles can be seen here for the cells at the front edge of the magnets (see the top image in figure 6). Eventually the cells move through the microchannel one by one and form a focused stream of about 20 μm wide downstream of the magnets (see the bottom image in figure 6). The experimental images

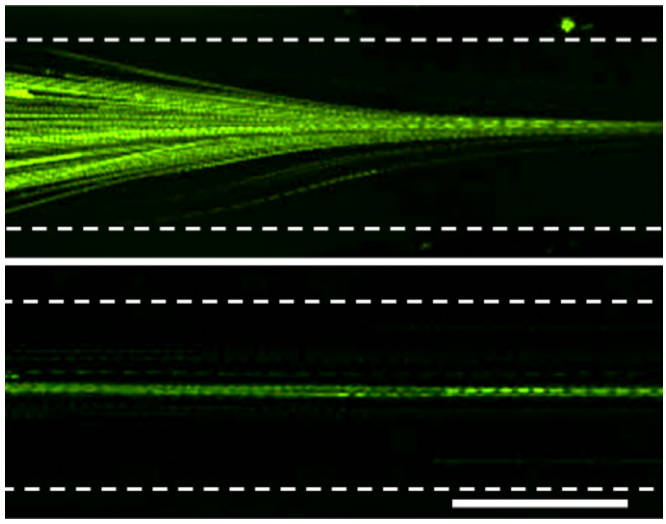

Figure 6. Experimentally obtained streak images show the magnetic focusing of yeast cells in ferrofluid at a mean flow speed of 0.4 mm s^{-1}. The images were obtained from the same view windows as explained in figure 3. The simulated cell trajectories are similar to those presented in figure 3(*a*) (bottom row) and not included here. The flow direction is from left to right in both images. The scale bar represents 600 μm.

agree with the simulated cell trajectories that are presented in figure 3(*a*) (bottom row).

A test for cell viability was performed using a spread plate technique, which enumerates and compares the total number of live yeast cells before and after magnetic focusing in the ferrofluid. In brief, a series of six tenfold dilutions were carried out for the cell suspension collected from the outlet reservoir after focusing experiment. A 100 μl of the dilution was plated in triplicates on Potato Dextrose agar plates and incubated at 30 °C for 24–48 h. Following that, the colonies were counted and the CFU ml^{-1} (Colony Forming Unit) was determined. The total number of cells counted was compared to that of the original cell suspension prior to being resuspended to ferrofluid for magnetic focusing test. Only a 10% decrease in the cell count was found, indicating a good biocompatibility of the demonstrated magnetic focusing method in ferrofluid.

5. Conclusions

We have developed an approach to embedding two opposing permanent magnets about a straight planar microchannel with good accuracy. The distance between the two magnets is determined solely by the size of the magnets involved in the fabrication process, which is 3.1 mm or 1/8″ for the tested microfluidic device. This device has been used to implement a three-dimensional magnetic focusing of 5 μm diamagnetic particles in ferrofluid at a mean flow speed of 0.4 mm s^{-1}, which is comparable to those reported in the literature [38–43]. Such focusing results from the negative magnetophoretic particle motion and is investigated through visualizations from both the top and side of the microchannel. We observe that particles exit the magnets region in a focused stream flowing near the centerline of the bottom channel wall, which is potentially useful to the electrical detection of particles through sensing electrodes deposited on the wall [9]. The effectiveness of this diamagnetic particle focusing in ferrofluid is enhanced when the flow speed is decreased and/or the particle size is increased. The latter has been demonstrated by differentially focusing a 5 μm and 1 μm particle mixture, indicating potential applications of the developed magnetic focuser to continuous concentration and filtration of particles by size. This device has also been tested for live yeast cells, which turns out to be biocompatible. Moreover, we have developed a three-dimensional analytical model, which predicts with a good agreement the observed particle and cell focusing behaviors at various conditions.

Acknowledgments

This work was supported by NSF CAREER program under grant CBET-1150670 (Xuan) and by Clemson University through the University Research Grant (Xuan and Tzeng) and the Creative Inquiry Program (Xuan).

References

[1] Huh D, Gu W, Kamotani Y, Grotgerg J B and Takayama S 2005 *Physiol. Meas.* **26** R73–98
[2] Pamme N 2007 *Lab Chip* **7** 1644–59
[3] Ateya D A, Erickson J S, Howell P B Jr, Hilliard L R, Golden J P and Ligler F S 2008 *Anal. Bioanal Chem.* **391** 1485–98
[4] Fu L M, Yang R J, Lin C, Pan Y and Lee G B 2004 *Anal. Chim. Acta* **507** 163–9
[5] Chang C, Huang Z and Yang R J 2007 *J. Micromech. Microeng.* **17** 1479–86
[6] Tsai C H, Hou H H and Fu L M 2008 *Microfluid Nanofluid* **5** 827–36
[7] Hong T F, Ju W J, Wu M C, Tai C H, Tsai C H and Fu L M 2010 *Microfluid Nanofluid* **9** 1125–33
[8] Lee H C, Hou H H, Yang R J, Lin C H and Fu L M 2011 *Microfluid Nanofluid* **11** 469–78
[9] Watkins N, Venkatesan B M, Toner M, Rodriguez W and Bashir R 2009 *Lab Chip* **9** 3177–84
[10] Chung T D and Kim H C 2007 *Electrophoresis* **28** 4511–20
[11] Godin J, Chen C, Cho S H, Qiao W, Tsai F and Lo Y H 2008 *J. Biophoton* **1** 355–76
[12] Mao X and Huang T 2008 *IEEE Nanotechnol. Mag.* **2** 22–7
[13] Xuan X, Zhu J and Church C 2010 *Microfluid Nanofluid* **9** 1–16
[14] Zhao Y, Fujimoto B S, Jeffries G D M, Schiro P G and Chiu D T 2007 *Opt. Express* **15** 6167–76
[15] Petersson F, Nilsson A, Jonsson H and Laurell T 2005 *Anal. Chem.* **77** 1216–21
[16] Shi J, Yazdi S, Lin S S, Ding X, Chiang I K, Sharp K and Huang T J 2011 *Lab Chip* **11** 2319–24
[17] Liang L, Qian S and Xuan X 2010 *J. Colloid Interface Sci.* **350** 377–9
[18] Yu C H, Vykoukal J, Vykoukal D M, Schwartz J A and Gascoyne P R C 2005 *J. Microelectromech. Syst.* **14** 480–7
[19] Chu H, Doh I and Cho Y 2009 *Lab Chip* **9** 686–91
[20] Bhagat A A S, Kuntaegowdanahalli S S and Papautsky I 2010 *Biomed. Microdevices* **12** 187–95
[21] Di Carlo D, Irimia D, Tompkins R G and Toner M 2007 *Proc. Natl Acad. Sci.* **104** 18892–7
[22] Choi S, Song S, Choi C and Park J K 2008 *Small* **4** 634–41
[23] Aoki R, Yamada M, Yasuda M and Seki M 2009 *Microfluid Nanofluid* **6** 571–6
[24] Leshansky A M, Bransky A, Korin N and Dinnar U 2007 *Phys. Rev. Lett.* **98** 234501
[25] Yang S, Kim J Y, Lee S J, Lee S S and Kim J M 2011 *Lab Chip* **11** 266–73
[26] Church C, Zhu J, Nieto J, Keten G, Ibarra E and Xuan X 2010 *J. Micromech. Microeng.* **20** 065011
[27] Zhu J and Xuan X 2009 *Electrophoresis* **30** 2668–75
[28] Gijs M A M 2004 *Microfluid Nanofluid* **1** 22–40
[29] Pamme N 2006 *Lab Chip* **6** 24–38
[30] Nguyen N T 2012 *Microfluid Nanofluid* **12** 1–16
[31] Liu C, Stakenborg T, Peeters S and Lagae L 2009 *J. Appl. Phys.* **105** 102011
[32] Erb R M and Yellen B 2009 *Nanoscale Magnetic Materials and Applications* ed J P Liu (New York: Springer) pp 563–90
[33] Gijs M A M, Lacharme F and Lehmann U 2010 *Chem. Rev.* **110** 1518–63
[34] Suwa M and Watarai H 2011 *Anal. Chim. Acta* **690** 137–47
[35] Zhu T, Marrero F and Mao L 2010 *Microfluid Nanofluid* **9** 1003–9
[36] Shen S, Hwang H, Hahn Y K and Park J K 2012 *Anal. Chem.* **84** 3075–81
[37] Vojtisek M, Tarn M D, Hirota N and Pamme N 2012 *Microfluid Nanofluid* **12** at press
[38] Afshar R, Moser Y, Lehnert T and Gijs M A M 2011 *Anal. Chem.* **83** 1022–9
[39] Liang L and Xuan X 2012 *Microfluid Nanofluid* **12** at press
[40] Peyman S A, Kwan E Y, Margarson O, Iles A and Pamme N 2009 *J. Chromatogr.* A **1216** 9055–62

[41] Rodriguez-Villarreal A I, Tarn M D, Madden L A, Lutz J B, Greenman J, Samitier J and Pamme N 2011 *Lab Chip* **11** 1240–8
[42] Zhu T, Cheng R and Mao L 2011 *Microfluid Nanofluid* **11** 695–701
[43] Kose A R and Koser A 2012 *Lab Chip* **12** 190–6
[44] Zhu J, Liang L and Xuan X 2012 *Microfluid Nanofluid* **12** 65–73
[45] Liang L, Zhu J and Xuan X 2011 *Biomicrofluid* **5** 034110
[46] Zhu T, Lichlyter D J, Haidekker M A and Mao L 2011 *Microfluid Nanofluid* **10** 1233–45
[47] Zhu T, Cheng R, Lee S A, Rajaraman E, Eiteman M A, Querec T D, Unger E R and Mao L 2012 *Microfluid Nanofluid* **12** at press
[48] Rosensweig R E 1985 *Ferrohydrodynamics* (Cambridge: Cambridge University Press)
[49] Furlani E P 2001 *Permanent Magnet and Electromechanical Devices: Materials, Analysis and Applications* (New York: Academic)